The Journal of Immunology

A Dynamic Variation of Pulmonary ACE2 Is Required to Modulate Neutrophilic Inflammation in Response to *Pseudomonas aeruginosa* Lung Infection in Mice

Chhinder P. Sodhi, Jenny Nguyen, Yukihiro Yamaguchi, Adam D. Werts, Peng Lu, Mitchell R. Ladd, William B. Fulton, Mark L. Kovler, Sanxia Wang, Thomas Prindle, Jr., Yong Zhang, Eric D. Lazartigues, Michael J. Holtzman, John F. Alcorn, David J. Hackam and Hongpeng Jia

J Immunol 2019; 203:3000-3012; Prepublished online 23 October 2019;
doi: 10.4049/jimmunol.1900579
http://www.jimmunol.org/content/203/11/3000

The Journal of Immunology is published twice each month by
The American Association of Immunologists, Inc.,
1451 Rockville Pike, Suite 650, Rockville, MD 20852

Print ISSN: 0022-1767 Online ISSN: 1550-6606.

A Dynamic Variation of Pulmonary ACE2 Is Required to Modulate Neutrophilic Inflammation in Response to *Pseudomonas aeruginosa* Lung Infection in Mice

Chhinder P. Sodhi,* Jenny Nguyen,† Yukihiro Yamaguchi,* Adam D. Werts,* Peng Lu,* Mitchell R. Ladd,* William B. Fulton,* Mark L. Kovler,* Sanxia Wang,* Thomas Prindle, Jr.,* Yong Zhang,‡ Eric D. Lazartigues,§,¶ Michael J. Holtzman,‡ John F. Alcorn,‖ David J. Hackam,* and Hongpeng Jia*

Angiotensin-converting enzyme 2 (ACE2) is a potent negative regulator capable of restraining overactivation of the renin–angiotensin system, which contributes to exuberant inflammation after bacterial infection. However, the mechanism through which ACE2 modulates this inflammatory response is not well understood. Accumulating evidence indicates that infectious insults perturb ACE2 activity, allowing for uncontrolled inflammation. In the current study, we demonstrate that pulmonary ACE2 levels are dynamically varied during bacterial lung infection, and the fluctuation is critical in determining the severity of bacterial pneumonia. Specifically, we found that a pre-existing and persistent deficiency of active ACE2 led to excessive neutrophil accumulation in mouse lungs subjected to bacterial infection, resulting in a hyperinflammatory response and lung damage. In contrast, pre-existing and persistent increased ACE2 activity reduces neutrophil infiltration and compromises host defense, leading to overwhelming bacterial infection. Further, we found that the interruption of pulmonary ACE2 restitution in the model of bacterial lung infection delays the recovery process from neutrophilic lung inflammation. We observed the beneficial effects of recombinant ACE2 when administered to bacterially infected mouse lungs following an initial inflammatory response. In seeking to elucidate the mechanisms involved, we discovered that ACE2 inhibits neutrophil infiltration and lung inflammation by limiting IL-17 signaling by reducing the activity of the STAT3 pathway. The results suggest that the alteration of active ACE2 is not only a consequence of bacterial lung infection but also a critical component of host defense through modulation of the innate immune response to bacterial lung infection by regulating neutrophil influx. ***The Journal of Immunology*****, 2019, 203: 3000–3012.**

Pneumonia remains a leading cause of morbidity and mortality from infectious disease worldwide (1–4). Although successful antimicrobial treatment can lead to recovery, pneumonia survivors may have reduced quality of life and are at increased risk of developing chronic lung disease (1, 5). Although viruses remain the most common pathogen causing pneumonia, both postviral bacterial superinfection and combined viral-bacterial coinfection are frequent occurrences and lead to more severe disease. Additionally, increasing antibiotic resistance patterns have made the treatment of bacterial pneumonia challenging. As such, bacterial pneumonia remains a significant public health concern (6–8). Although bacterial infection alone can initiate lung injury, it is the host-defense response that results in exaggerated inflammation and results in further lung injury and delayed recovery (9–11). Therefore, an improved understanding of the mechanisms underlying the host/pathogen interactions in bacterial pneumonia is imperative to develop new therapeutic strategies that balance the need for an adequate host defense with an injurious inflammatory response.

The renin–angiotensin system (RAS) regulates blood pressure, fluid dynamics, and electrolyte balance (12). Additionally, it plays a role in modulating the innate immune system and is a potent regulator of inflammation (13). RAS components are expressed in many tissues and cells, including the lung (14, 15). The system

*Division of Pediatric Surgery, Department of Surgery, Johns Hopkins University School of Medicine, Baltimore, MD 21205; †Department of Bioengineering, School of Engineering and Applied Sciences, University of Pennsylvania, Philadelphia, PA 19104; ‡Division of Pulmonary and Critical Care Medicine, Department of Medicine, Washington University School of Medicine, St. Louis, MO 63110; §Department of Pharmacology and Experimental Therapeutics, School of Medicine, Louisiana State University Health Sciences Center, New Orleans, LA 70112; ¶Southeast Louisiana Veterans Health Care System, New Orleans, LA 70119; and ‖Division of Pulmonary Medicine, Department of Pediatrics, University of Pittsburgh Medical Center Children's Hospital of Pittsburgh, University of Pittsburgh, Pittsburgh, PA 15224

ORCIDs: 0000-0003-3988-2912 (Y.Y.); 0000-0002-8977-5704 (A.D.W.); 0000-0001-5312-8452 (M.R.L.); 0000-0002-4133-4483 (S.W.); 0000-0001-7290-0786 (E.D.L.).

Received for publication May 31, 2019. Accepted for publication September 26, 2019.

This work was supported by grants from the National Institutes of Health, National Institute of Allergy and Infectious Diseases (U19-AI070412, R01-AI111605, and R01-AI130591) and the National Heart, Lung, and Blood Institute (R01-HL121791, R01-HL120153, and UH3-HL107183) (to Y.Z. and M.J.H.). M.R.L. received salary support during his contribution to this study under a National Institutes of Health, National Institute of Diabetes and Digestive and Kidney Diseases T32 training grant (2T32DK007713-21). A.D.W. is supported by a training grant (T32 OD011089). E.D.L. was supported, in part, by research grants from the National Institutes of Health (HL093178), the Department of Veterans Affairs (BX004294), and the Research Enhancement Program at the Louisiana State University Health Sciences Center, New Orleans.

Address correspondence and reprint requests to Dr. Hongpeng Jia, Division of Pediatric Surgery, Department of Surgery, Johns Hopkins University, 472 Miller Research Building, 733 North Broadway, Baltimore, MD 21205-1832. E-mail address: hjia4@jhmi.edu

The online version of this article contains supplemental material.

Abbreviations used in this article: ACE2, angiotensin-converting enzyme 2; $ACE2^{ko}$, ACE2 knockout; BALF, bronchoalveolar lavage fluid; dpi, day postinoculation; iNOS, inducible NO synthase; KS, kinin system; L.B., Luria–Bertani; RAS, renin–angiotensin system; rhACE2, recombinant human ACE2.

is activated during bacterial pneumonia infection to maintain blood pressure and mount the host-defense response (16, 17). However, unrestrained RAS activation prolongs inflammation, resulting in further lung damage. Moreover, the RAS directly influences the kinin system (KS), which is also activated during bacterial lung infection and leads to increased lung inflammation (18, 19). Thus, limiting the overactivation of both the RAS and KS represents an attractive therapeutic strategy for modulating the harmful hyperinflammatory response to bacterial infection in the lung.

Angiotensin-converting enzyme 2 (ACE2) is a terminal carboxypeptidase that functions to regulate both the RAS and KS by converting its substrates to either active or inactive metabolites (20). Specifically, ACE2 functions as a potent negative regulator of RAS-induced inflammation mainly because of its action converting Ang II to Ang 1–7 (21, 22), which results in inhibition of Ang II/AGT1R signaling and activating the Ang 1–7/Mas1 axis. Thus, ACE2 acts to shift RAS activity from proinflammatory to anti-inflammatory states. Additionally, ACE2 temporizes inflammation produced by the KS, where it inactivates Des-Arg^9 bradykinin (DABK), thus inhibiting DABK-mediated inflammation (23, 24). Therefore, ACE2 could regulate the inflammatory response by limiting the overactivation of both RAS and KS, which makes ACE2 an ideal therapeutic target for treating and preventing lung damage caused by an overactive inflammatory response in bacterial pneumonia. In fact, in other diseases such as sepsis and acid aspiration–induced lung injury, ACE2 has been shown to be beneficial in modulating the inflammatory response (21, 25), and studies have shown that pulmonary ACE2 is impaired in several lung diseases, including viral and aspiration pneumonia, pulmonary hypertension, and LPS-induced lung injury (20, 26–28). However, the role of ACE2 in bacterial lung infection remains poorly understood, and the potential role of ACE2 in the pathogenesis of, and defense against, bacterial pneumonia has not been established.

In this study, we explored the novel link between ACE2 activity and the innate immune response in a mouse model of bacterial pneumonia. We hypothesized that ACE2 plays a critical, but previously unrecognized, role in balancing the inflammatory-immune response to bacterial lung infection, in part through modulating neutrophil infiltration.

Materials and Methods

Reagents and Abs

The ACE2 inhibitor MLN4760 was purchased from AnaSpec (Freemont, CA). Recombinant human ACE2 (rhACE2) is a product from R&D Systems (Minneapolis, MN). Mouse rIL-17A is a product by PeproTech (Rocky Hill, NJ). STAT3 inhibitor WP1066 was purchased from Santa Cruz Biotechnology (Dallas, TX). All Ab information is listed in Table I.

Study approval

Mice. The animal experiments described in these studies were approved by the Johns Hopkins University Animal Care and Use Committee (protocol number M017M304) and were performed according to the Guide for the Care and Use of Laboratory Animals of the National Institutes of Health. Eight- to sixteen-week-old male and female C57BL/B6 mice were obtained from The Jackson Laboratory and bred and housed in the Johns Hopkins University animal facility.

To generate a mouse line in which the ACE2 gene was precisely excised from Foxj1$^+$ lung epithelial cells (ACE2$^{\Delta Foxj1}$), *ACE2*^{loxP} mice were generated by Dr. E. Lazartigues (Louisiana State University, New Orleans, LA) using embryonic stem cells (project identification CSD79596) obtained from the Knockout Mouse Project (University of California, Davis, Davis, CA) and cross-bred with Foxj1^{cre} mice (Dr. Michael Holtzman's Lab, Washington University, St. Louis, MO) (29). The progeny were found to be lacking ACE2 expression in the specific type of cells, as determined by immunohistochemistry and reduced ACE2 activity in bronchoalveolar lavage fluid (BALF) (Supplemental Fig. 2). Global ACE2 knockout (ACE2^{ko}) are a generous gift from Dr. J. Penninger of Institute of Molecular Biotechnology, Austria.

Mouse lung organoid culture

Establishment of lung organoid cultures followed a published protocol with minor modification (30). In brief, mouse lungs were diced, and the tissue was subjected to cell separation using Liberase (2 μg/ml; Roche), followed by mechanical dissociation (21-gauge needle) and DNA digestion (DNase I, 120 μ/ml; Roche). They were then maintained for 10–12 d before experiments were conducted. Organoids were grown on Matrigel and supplied with DMEM/F12 containing 5% FBS, penicillin/streptomycin (100 U/ml), glutamine (1%), amphotericin B (1×), insulin/transferrin/selenium (1×, no. 15290018; Life Technologies), recombinant mouse EGF (0.025 μg/ml, no. SRP3196; Sigma-Aldrich), cholera toxin (0.1 μg/ml, no. C8052; Sigma-Aldrich), and bovine pituitary extract (30 μg/ml, no. P1476; Sigma-Aldrich). All-trans retinoic acid was freshly added to organoid culture media (0.01 μM, no. R2625; Sigma-Aldrich) A ROCK inhibitor, Y-27632 (10 μM, no. 1254; Tocris Bioscience), was added for the first 48 h of culture.

Flow cytometry for neutrophils

Flow cytometry was performed in single-cell suspensions from mouse BALF as reported previously (31). The pellet was then resuspended in 10 ml 1% BSA (VWR Life Sciences) in PBS and centrifuged at 400 × *g*, 4°C for 5 min, and the supernatant was discarded. The cell pellet was resuspended at 2.5 × 10^7 cells/ml in FACS buffer. Single-cell suspensions were then incubated with anti-CD16/CD32 (BD Biosciences) to block Fc receptor binding (20 min at 4°C). Neutrophils were gated as 7AAD$^-$Ly-6G$^+$CD11b$^+$ and analyzed according to the manufacturer's guidance on a BD Accuri C6 flow cytometer. All Abs used are listed in Table I.

Lung wet/dry ratio measurement

Mouse lungs from each experimental group were collected, and a portion of the lungs was assessed for wet/dry ratio measurement. Briefly, mouse lungs were removed, and wet weights were measured, followed by placement of the lung tissue in an incubator at 65°C for 72 h. The dry weights of lung tissues were measured, and the wet/dry ratio was calculated to evaluate lung edema: wet-to-dry = wet weight/dry weight.

Immunohistochemistry, immunofluorescence, and SDS-PAGE

Immunofluorescent staining of lung tissues was performed on 4% paraformaldehyde-fixed 5-μm paraffin sections. The sections were first warmed to 56°C in a vacuum incubator (Isotemp Vacuum Oven; Thermo Fisher Scientific) then washed immediately twice with xylene, gradually redehydrated in ethanol (100, 95, and 70% and water), and then processed for Ag retrieval in citrate buffer (10 mM [pH 6])/microwave (1000 W, 6 min). Samples were then washed with PBS, blocked with 1% BSA/5% donkey-serum (1 h, room temperature), then incubated overnight at 4°C with primary Abs (1:200 dilutions in 0.5% BSA), washed three times with PBS, incubated with appropriate fluorescent-labeled secondary Abs (1:1000 dilution in 0.5% BSA; Life Technologies) as well as the nuclear marker DAPI (BioLegend), and slides were then mounted using Gelvatol (Sigma-Aldrich) solution prior to imaging using a Nikon Eclipse Ti confocal microscope (Nikon) under appropriate filter sets. Abs used in mouse lung immunostainings are cleaved caspase 3 (rabbit anti-rat/mouse; Biocare Medical), DAPI (Life Sciences), and inducible NO synthase (iNOS; mouse anti-rat/mouse; BD Biosciences). SDS-PAGE was performed as in (32, 33), in which tissue samples were collected in radioimmunoprecipitation assay buffer (no. BP-115; Boston BioProducts) containing phosphatase and protease inhibitor mixture (no. BP-480; Boston BioProducts; no. PIC02; Cytoskeleton), and homogenized with homogenizing beads on a BeadBlaster (Benchmark Scientific) and centrifuged at 4°C at 16,000 × *g* for 5 min. Supernatants were collected, and equal amounts of protein were loaded on SDS-PAGE gel before transferring to a cellulose membrane for Ab detection.

Measurement of catalytic activity of ACE2

ACE2 activity in BALF was determined by measuring the fluorescence intensity of ACE2 substrate Mca-YVADAPK(Dnp)-OH (catalog no. ES007; R&D Systems) (34). In brief, samples were diluted in assay buffer (50 mM MES, 300 mM NaCl, 10 nM $ZnCl_2$, and 0.01% Brij-35 [pH 6.5]) and incubated with ACE2 substrate, with or without the ACE2 inhibitor MLN4760 (1 nM, catalog no. 62337; AnaSpec), at 37°C for 45 min. The fluorescence intensity was determined using a multiplate fluorescence reader at excitation 320 nm and emission 405 nm.

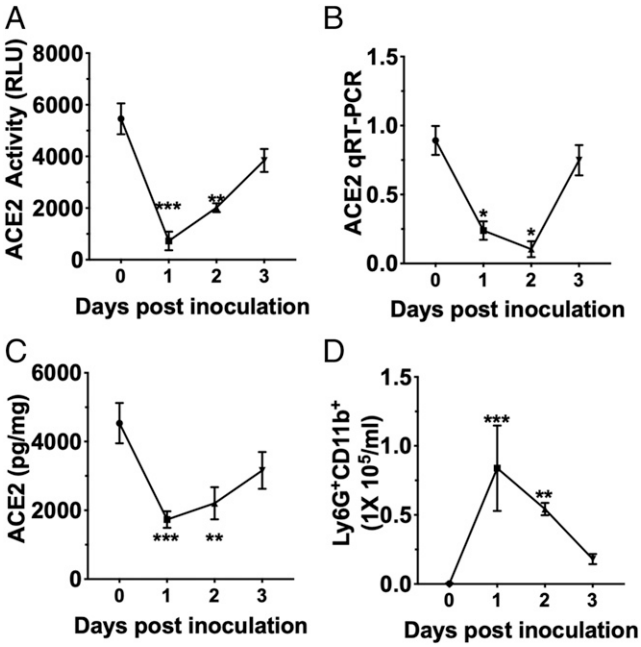

FIGURE 1. Pulmonary ACE2 expression and activity are dynamically variable in response to *P. aeruginosa* infection. A bacterial pneumonia model was established by instilling 30 μl saline containing 1×10^6 *P. aeruginosa* (Pao1 strain) through intubation with an otoscope. At time after bacterial inoculation, mice were sacrificed, and BALF or lung tissues were collected. (**A**) ACE2 activity in BALF was measured by fluorescent substrate (Fluro-substrate)–based assay. The relative light unit or relative luminescence unit (RLU) was normalized by recovery volume of respective BALF. The ACE2 gene expression level was measured by quantitative RT-PCR and displayed as ACE2 mRNA expression level relative to a housekeeping gene RPLO mRNA expression level (**B**), and ACE2 protein level in mouse lung homogenates was determined by ELISA, and the concentration was normalized by protein concentration (**C**). (**D**) Neutrophil numbers in BALF were determined by flow cytometry and gated as Ly-6G$^+$CD11b$^+$ in live cells (7AAD$^-$). In all samples, $n \geq 5$. All comparisons were done between the nontreated group (0) and treated group at the time (day) of sacrifice after bacterial inoculation. Data were analyzed for statistical significance by two-tailed Student *t* test or ANOVA (ordinary one-way ANOVA multiple comparisons) using Prism software (GraphPad). $*p < 0.05$, $**p < 0.01$, $***p < 0.001$.

Detection of mRNA expression by quantitative RT-PCR

Total RNA was isolated from mouse lung tissue and reverse transcribed using the QuantiTect Reverse Transcription Kit (QIAGEN). The expression levels of mouse ACE2 were determined relative to the housekeeping gene *RPL0* by quantitative real-time PCR using the Bio-Rad Laboratories CFX96 real-time system, as described previously (33). The following primers were used to detect individual mRNA levels: mouse ACE2 forward: 5′-TCTGCCACCCCACAGCTT-3′, reverse 5′-GGCTGTCAAGAAGTTGTCCATTG-3′; and mouse RPL0 forward primer: 5′-GGCGACCTGGAAGTCCAACT-3′, reverse 5′-CCATCAGCACCACAGCCTTC-3′.

ELISA

Sandwich ELISA analysis for mouse ACE2 was performed according to the manufacturer's instructions (Innovative Research catalog no. IRKTAH5291). Briefly, a capture Ab of mouse ACE2 has incubated in 96-well flat-bottom plates overnight. Plates were washed and blocked with 5% BSA (1 h, room temperature) and samples were added to the plate, incubated overnight (4°C), and washed extensively then incubated with a biotinylated anti-mouse ACE2 detection Ab (2 h at room temperature). Following washes, the streptavidin/alkaline phosphatase was added to the wells and incubated at room temperature for 20 min. Then, the plate was washed again as described above, and a substrate solution (color reagent A and B with 1:1 ratio; R&D Systems) was added, and the enzymatic reaction was stopped after 30 min by the addition of an equal volume of 0.2 N sulphuric acid, and the color change was read on a spectrophotometer (450 nm; Molecular Dynamics). Data were normalized to total protein concentration and analyzed using GraphPad (Prism). Protein contents in BALF were determined by BCA assay (no. 23225; Pierce). Murine CXCL5, keratinocyte chemoattractant (KC) or Cxcl1, MiP2, and G-CSF abundances were assessed by ELISA (R&D Systems) following the manufacturer's instructions.

Growth of Pseudomonas aeruginosa *bacteria*

P. aeruginosa (Pao1 strain, kindly gifted from Dr. P. B. McCray, University of Iowa) were stocked at −80°C. Two days before the experiment, bacteria were streaked on a Luria–Bertani (L.B.) plate and incubated at 37°C overnight. A single colony was picked and cultured in L.B. broth at 37°C overnight. On the day of the experiment, overnight cultured *Pseudomonas* were transferred to a new culture tube containing fresh L.B. broth in a 1:100 ratio. Four to six hours postinoculation, cultures were checked with a spectrometer at 595 nM to determine the density of bacteria content as such: OD 595 = 0.1 equals to 1×10^8 CFU/ml.

P. aeruginosa *induced bacterial pneumonia model*

Mice 6–12 wk of age were anesthetized by i.p. injection of ketamine/xylazine (87.5 ± 2.5/10 mg/kg). A mouse model of bacterial pneumonia was established by the intratracheal administration of 1×10^6/30 μl *P. aeruginosa* (Pao1 stain) via tracheal intubation. For tracheal administration of reagents, mice were first anesthetized by inhaled isoflurane and then administered by nasal inhalation either rhACE2 (10 μg/kg), the ACE2 inhibitor MLN4760 (2.5 mg/kg), or the STAT3 inhibitor WP1066 (10 μg/kg) in 50 μl of total volume. For neutralizing or blocking experiments, isotype control rat IgG (25 mg/kg), rat anti–Ly-6G mAb, isotype rabbit IgG (25 mg/kg), or rabbit anti–IL-17 Ab was dissolved in 50 μl saline and

Table I. List and application of Abs

Ag	Primary Ab	Secondary Ab	Application	Vendor
ACE2	Rat	Donkey	IF	R&D Systems
Actin	Mouse (HRP)		Western blot	GenScript
Aqp3	Rabbit	Donkey	IF	Abcam
CC3	Rabbit	Donkey	IF	Biocare Medical
CD11b	Rat		Glow cytometry	BioLegend
Foxj1	Mouse	Donkey	IF	eBioscience
IL-17A	Goat	Donkey	Neutralization	R&D Systems
iNOS	Mouse	Donkey	IF	BD Biosciences
Ly-6G	Rat		Flow cytometry	BioLegend
Ly-6G	Rat		Depletion	R&D Systems
MPO	Goat	Donkey	IF	Santa Cruz Biotechnology
Muc5A	Mouse	Donkey	IF	Thermo Fisher Scientific
p-STAT3	Rabbit	Goat	Western blot	Cell Signaling Technology
PdPn	Rabbit	Donkey	IF	Abbiotec
Pgp9.5	Mouse	Donkey	IF	Abcam
Scgb1A1	Rabbit	Donkey	IF	MilliporeSigma
STAT3	Rabbit	Goat	Western blot	Cell Signaling Technology

IF, immunofluorescence; MPO, myeloperoxidase.

Table II. Pathologic score system adopted from the American Thoracic Society guideline

Parameter	Score per Field		
	0	1	2
A. Neutrophils in the alveolar space	None	1–5	>5
B. Neutrophils in the interstitial space	None	1–5	>5
C. Hyaline membranes	None	1	>1
D. Proteinaceous debris filling the airspaces	None	1	>1
E. Alveolar septal thickening	<2×	2×–4×	>4×

administered by nasal inhalation at 2 h before and 24 h after bacterial inoculation.

Neutrophil depletion

Mice were administered 5 mg/kg of either rat mAb anti–Ly-6G, clone 1A8, or isotope rat IgG by nasal inhalation 24 h after bacterial inoculation. Neutrophil counts in BALF were determined by flow cytometry as gated as $7AAD^-$ $Ly\text{-}6G^+CD11b^+$.

Bronchoalveolar lavage

Mice were euthanized, and a midline incision was performed to open the chest. The lungs were lavaged in situ via PE-90 tubing inserted into the exposed trachea. Lavage was carried out with 0.5-ml volumes of sterile saline (total lavage volume 2 ml/mouse). The recovered volumes of each BALF sample were recorded to normalize protein concentration in BALF. Protein contents in BALF were determined by bicinchoninic acid assay (no. 23225; Pierce).

Bacterial load in BALF

To measure bacterial load in samples, BALF was serially diluted (1:10) in sterile PBS. Ten microliters from each dilution were plated onto separate L.B. agar plates, and the plates were incubated at 37°C for 18 h. Two replicates of each dilution were plated on L.B. agar plates. Colonies were counted separately for each sample. Bacterial load was displayed as CFU per milliliter in BALF.

Histologic lung injury score

To quantify the extent of histologic lung injury, we adopted the American Thoracic Society recommended scoring system as shown in Table II:

$$\text{Score} = [(20 \times A) + (14 \times B) + (7 \times C) + (7 \times D) + (2 \times E)]/(\text{number of fields} \times 100)$$

The scores were recorded by two independent researchers who do not participate in the experimental procedures, nor did they know the content of each H&E slide they scored. At least five fields of each slide were scored.

Statistical analysis

Where indicated, data were analyzed for statistical significance by two-tailed Student *t* test or ANOVA (ordinary one-way ANOVA multiple comparisons) using Prism software (GraphPad). Statistical significance was determined as having a value <0.05, and data are represented as mean ± SEM as indicated. All experiments were repeated at least twice, with at least three mice per group for assessment.

Results

Pulmonary ACE2 expression and activity are dynamically variable in response to P. aeruginosa *infection*

Previously, we demonstrated that administration of bacterial LPS into mouse lung attenuated pulmonary ACE2 activity dynamically (28). To study whether pulmonary ACE2 plays a similar role in the pathogenesis of bacterial pneumonia, we established a mouse model by intratracheal instillation of 1×10^6/30 μl *P. aeruginosa* via tracheal intubation. As we have previously reported, enzymatically active pulmonary ACE2 is shed from the airway epithelium

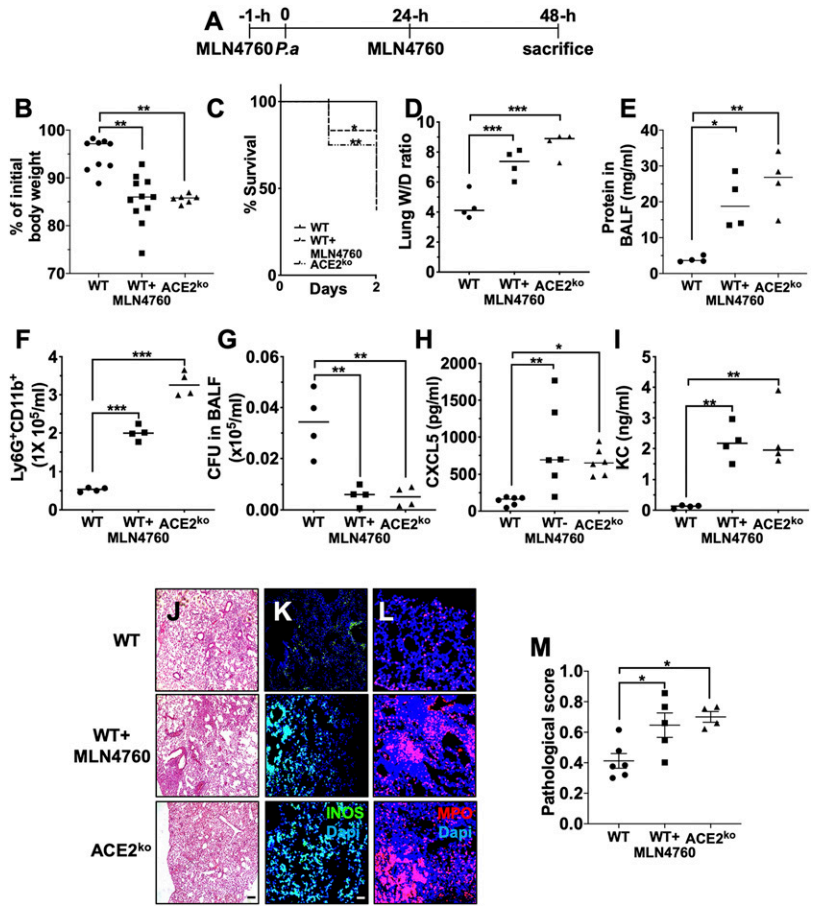

FIGURE 2. Pre-existing and persistent lack of the active ACE2 exacerbates the severity and worsens the prognosis of bacterial pneumonia. (**A**) Schematic depicting the strategy of ACE2 inhibitor (MLN4760; 2.5 mg/kg) treatment. (**B**) Bodyweight change at the time of sacrifice. (**C**) Survival curve of mice in respective experimental groups as indicated. (**D**) The degree of lung permeability from mice of respective experimental groups was determined by wet/dry ratio. (**E**) Levels of total protein in BALF from mice of the indicated experimental group. (**F**) Neutrophil accumulation in mouse lungs with pre-existing and persistent deficiency of the active ACE2 was assayed by flow cytometry gated as $Ly\text{-}6G^+CD11b^+$ living cells in BALF. (**G**) Bacterial load in mouse BALF was determined by CFU. The volume of individual BALF normalized the CFU (indicated as CFU per milliliter). (**H** and **I**) Proinflammatory cytokine and chemokine levels of CXCL5 and KC were determined by ELISA. (**J**) Representative micrograph of pathohistology of lungs from indicated groups at the time after bacterial inoculation. (**K** and **L**) Representative immunofluorescence images from an indicated experimental group of mice for iNOS (K), and neutrophil marker myeloperoxidase (MPO) (L). (**M**) Pathological scores of mouse lungs from wild-type mice with or without MLN4760 treatment and $ACE2^{ko}$ mice were calculated. Data were analyzed for statistical significance by two-tailed Student *t* test or ANOVA (ordinary one-way ANOVA multiple comparisons) using Prism software (GraphPad). In all experiments, $n \geq 4$. Scale bar, 50 μm. $*p < 0.05$, $**p < 0.01$, $***p < 0.001$.

after inoculation with LPS (27). Therefore, we first measured ACE2 enzymatic activity in BALF from bacterially infected mouse lung. We found that ACE2 activity is suppressed significantly in the first 2 d after bacterial inoculation, but increases beginning 3 d postinoculation (dpi) (Fig. 1A), explaining the dynamics of ACE2 gene and protein expression in the lung (Fig. 1B, 1C). This suggests a correlation between bacterial infection and various levels of active pulmonary ACE2. Similar to what we observed in the LPS-induced lung injury model (28), the time-sensitive variation in pulmonary ACE2 production and activity in our bacterial pneumonia model is inversely related to the number of neutrophils in BALF (Fig. 1D). The above observation led us to consider whether the dynamics of ACE2 activity are responsible for the host-defense response to bacterial insult and that variation in pulmonary ACE2 is not only a consequence of bacterial lung infection, but also a driving force for inflammatory cell recruitment (Tables I, II).

Pre-existing and persistent deficiency of active ACE2 exacerbates the severity and worsens the prognosis of bacterial pneumonia

To address the above question, we manipulated pulmonary ACE2 activity by giving the mice either the ACE2 inhibitor MLN4760 or rhACE2 through inhalation to disrupt ACE2 dynamics. First, we reduced pulmonary ACE2 activity of adult wild-type mice through the administration of the ACE2 inhibitor, MLN-4760 (2.5 mg/kg), via nasal inhalation. This manipulation was done both before and 24 h after bacterial inoculation (Fig. 2A). We found that reduction in ACE2 activity led to exaggerated lung injury, as evidenced by increased weight loss (Fig. 2B), reduced survival (Fig. 2C), increased lung permeability as manifested by elevated lung wet/dry ratio (Fig. 2D), and by more protein content in BALF (Fig. 2E). Interestingly, mice that received an ACE2 inhibitor demonstrated enhanced neutrophil accumulation in the air space of the lung (Fig. 2F) and a remarkably reduced bacterial burden (Fig. 2G), suggesting that the increased disease severity after inhibition of pulmonary ACE2 was due to exuberant neutrophil infiltration and not an overwhelming bacterial infection. The above concept is supported by elevated proinflammatory cytokine and chemokine levels in BALF (Fig. 2H, 2I), worsened histopathology (Fig. 2J, 2M), more severe parenchymal inflammation (Fig. 2K), and increased neutrophil accumulation in the parenchyma (Fig. 2L) in mice subjected to pulmonary ACE2 inhibition. To further confirm this observation, we subjected a global $ACE2^{ko}$ mouse to our model. Similar to wild-type mice who received an ACE2 inhibitor, $ACE2^{ko}$ mice showed increased inflammation, more severe lung injury, and decreased survival (Fig. 2B–M).

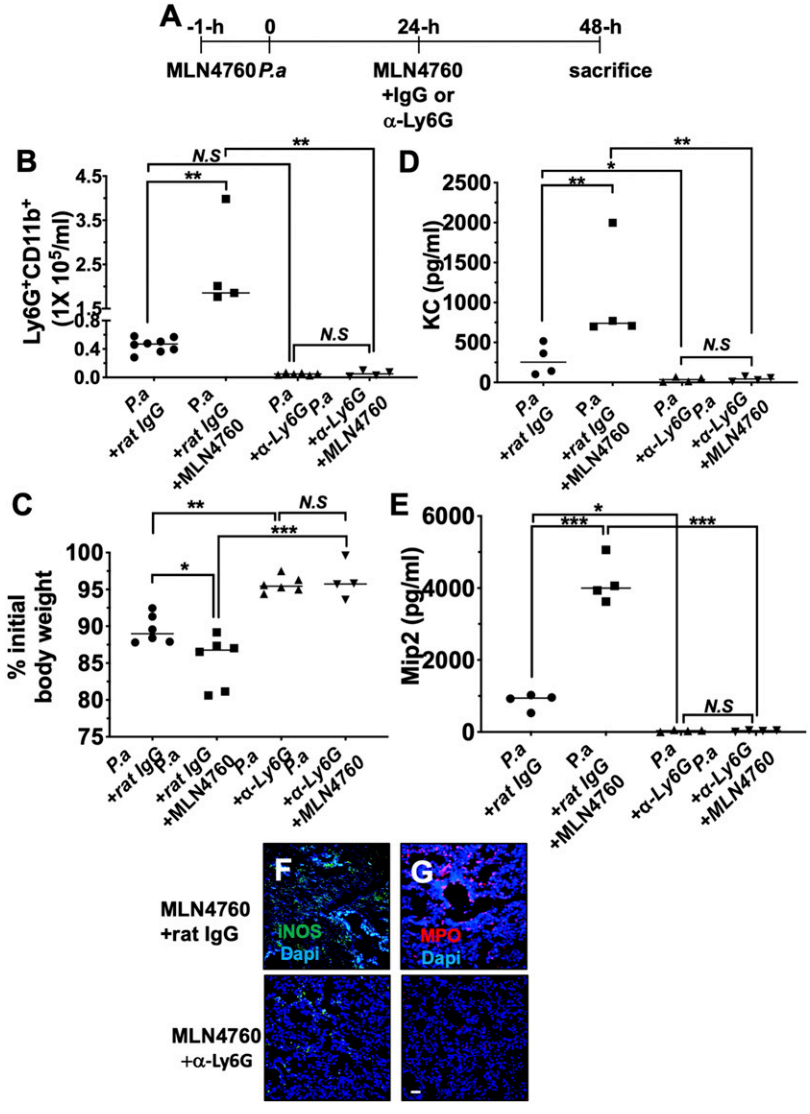

FIGURE 3. Deficiency of active ACE2-induced lung injury is due to heightened neutrophilic inflammation. (**A**) Schematic elaborating the strategy of ACE2 inhibitor (MLN4760; 2.5 mg/kg) and anti–Ly-6G (5 mg/kg) rat Ab treatment. (**B**) Neutrophil counts in BALF from experimental groups were determined by flow cytometry gated as live Ly-$6G^+CD11b^+$ cells. (**C**) Bodyweight changes 48 h after bacterial lung infection in comparison with initial bodyweight. (**D** and **E**) Levels of proinflammatory cytokine and inflammatory cell recruiting chemokine in BALF from experimental groups as indicated were detected by ELISA. Final concentrations were normalized by recovery volume. (**F** and **G**) Representative micrograph demonstrating immunofluorescent staining for inflammation marker iNOS (green) and neutrophil marker myeloperoxidase (MPO; red) in lung sections from mice as indicated. Data were analyzed for statistical significance by two-tailed Student *t* test or ANOVA (ordinary one-way ANOVA multiple comparisons) using Prism software (GraphPad). For each experimental group, $n \geq 4$. Scale bar, 50 μm. $*p < 0.05$, $**p < 0.01$, $***p < 0.001$. N.S, no statistical significance.

The active ACE2 deficiency–mediated excessive lung inflammation in response to bacterial lung infection is due to exuberant neutrophil accumulation in the lung

Next, we sought to elaborate the mechanism by which reduced pulmonary ACE2 activity led to increased neutrophil infiltration and subsequent inflammation. To do so, we again subjected mice to inhalation of the ACE2 inhibitor MLN4760 before bacterial inoculation (Fig. 3A) but added either a neutrophil depleting Ab (anti–Ly-6G) or control rat IgG with the second dose of MLN4760 that was given 24 h after bacterial lung inoculation. As shown in Fig. 3B–G, neutrophil depletion reversed the lung injury exacerbated by inhibition of pulmonary ACE2, as evidenced by significantly reduced neutrophil influx (Fig. 3B), the reversal of weight loss (Fig. 3C), alleviated inflammation (Fig. 3D, 3E), and reduced parenchymal inflammation and neutrophil accumulation (Fig. 3F, 3G). Taken together, these experiments strongly suggest that inhibition of active ACE2 leads to excessive lung inflammation in response to bacterial lung infection because of exuberant neutrophil accumulation in the lung.

Interrupting active ACE2 recovery attenuates the resolution of lung inflammation in bacterial pneumonia

As shown in Fig. 1, pulmonary ACE2 activity starts to recover 3 d after bacterial lung infection. We next asked whether interruption of ACE2 recovery will have an impact on the resolution of neutrophilic lung inflammation and injury. To address this question, we inhibited ACE2 activity starting at 3 dpi by giving the mice an ACE2-inhibitor MLN4760 through nasal inhalation and one dose daily after that (Fig. 4A). At 6 dpi, the mice were sacrificed and checked for markers of inflammation and injury. As demonstrated, persistent and prolonged lung inflammation and injury were observed in the lungs of mice who received MLN4760, which was manifested by impaired weight recovery (Fig. 4B), persistent neutrophil accumulation (Fig. 4C), elevated chemokine and cytokine concentration in BALF (Fig. 4D, 4E) and parenchymal pathology, and inflammation and neutrophil accumulation (Fig. 4F–H) in the lungs. However, almost complete resolution of inflammation and recovery from injury were achieved in the lungs of mice without ACE2 inhibitor, indicating that attenuating the recovery of ACE2 activity impairs the resolving process of inflammation and injury in bacterial pneumonia. This further underscores the critical role of ACE2 in the pathogenesis of lung inflammation in the experimental disease setting.

Preventing the pulmonary ACE2 reduction leads to impaired neutrophil recruitment, increased bacterial burden, and enhanced mortality in bacterial pneumonia

Previous reports illustrated that enhancing pulmonary ACE2 activity is beneficial to the hosts who encountered infectious or noninfectious insults in the lung (25, 28, 35–39). To verify that such beneficial effect of ACE2 in our bacterial lung infection model, as depicted in Fig. 5A, we supplied adult wild-type mice with rhACE2 (10 μg/kg by nasal inhalation) 2 h before and 24 h after *P. aeruginosa* inoculation. Surprisingly, we did not observe the beneficial effect of rhACE2 as reported by others. Instead, rhACE2 supplementation resulted in more severe mortality and further bodyweight loss in surviving mice (Fig. 5B, 5C), which was accompanied by high bacterial load and reduced proinflammatory neutrophil accumulation in BALF (Fig. 5D, 5E). Furthermore, such rhACE2 treatment led to compromised inflammatory response, as evidenced by reduced inflammatory chemokine and cytokine products in BALF (Fig. 5F–I), more severe histopathology of the lung (Fig. 5J), reduced parenchymal inflammation, and neutrophil accumulation (Fig. 5K, 5L). The results suggested that interfering with the dynamic variation of pulmonary ACE2 is detrimental to the host by compromising the innate host-defense capability to bacterial lung infection because, in part, of the impaired pulmonary neutrophil influx.

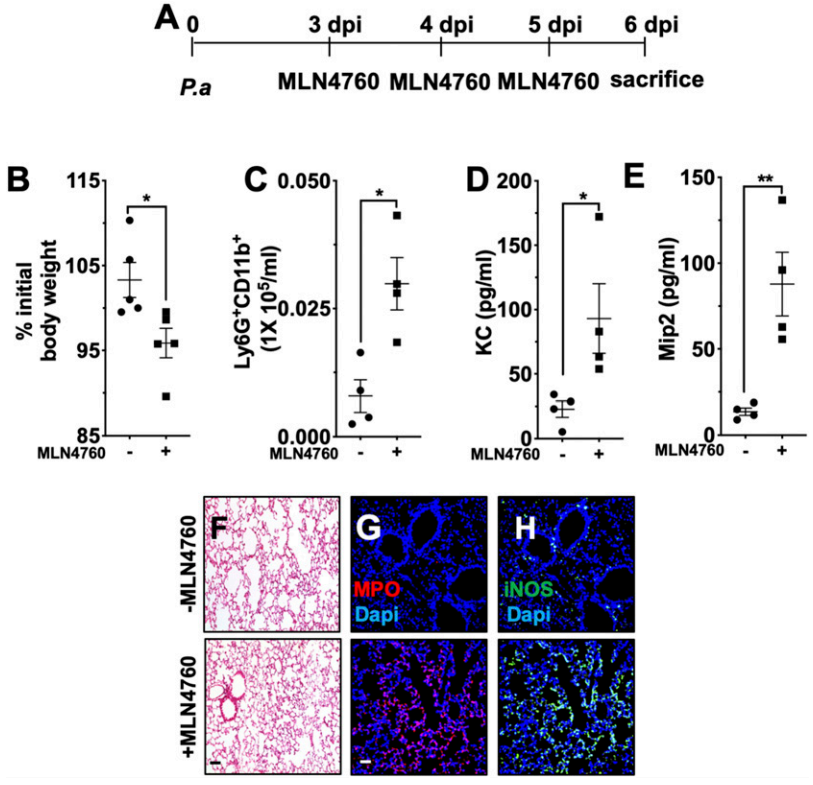

FIGURE 4. Interrupting active ACE2 recovery attenuates the resolution of lung inflammation in bacterial pneumonia. (**A**) Timelines outline the experimental protocol. (**B**) Bodyweight changes relative to initial bodyweight at 6 dpi with or without interrupting active ACE2 recovery by ACE2 inhibitor MLN4760. (**C**) Neutrophil accumulation in mouse lung infected by bacteria as manifested by live Ly-6G$^+$CD11b$^+$ cells in BALF using flow cytometry. (**D** and **E**) Interrupting active ACE2 recovery prolonged elevated proinflammatory cytokine (Mip2 and KC) levels in BALF determined by ELISA. (**F**) H&E staining micrograph showing histology of mouse lung with perturbed active ACE2 recovery at 6 dpi. (**G** and **H**) Representative micrograph demonstrating immunofluorescence for neutrophil marker myeloperoxidase (MPO; red) (G) and inflammation marker iNOS (green) (H) in lung sections from mice as indicated. Data were analyzed for statistical significance by two-tailed Student *t* test using Prism software (GraphPad). For each experimental group, $n \geq 4$. Scale bar, 50 μm. $^*p < 0.05$, $^{**}p < 0.01$.

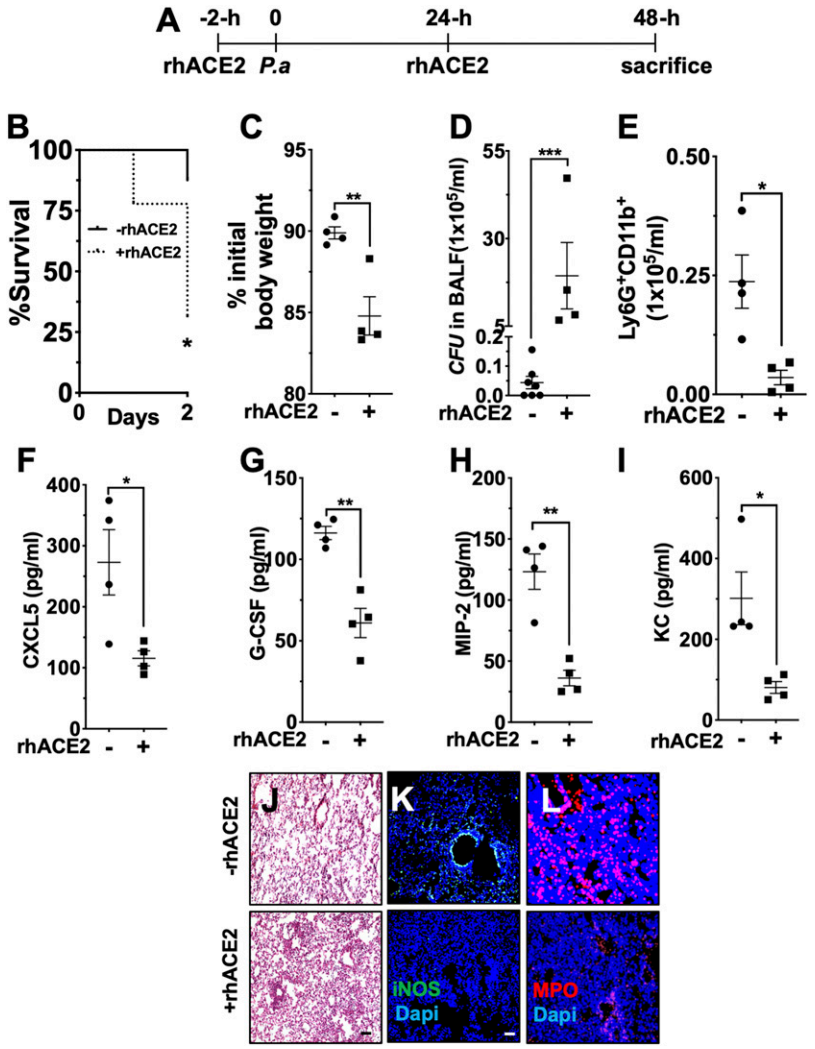

FIGURE 5. Precluding the active ACE2 reduction leads to impaired neutrophil recruitment, exuberant bacterial burden, and enhanced mortality in bacterial pneumonia. (**A**) Schematic depicting the strategy of recombinant ACE2 treatment. (**B**) The percentage of survived mice with or without rhACE2 at 2 d after bacterial lung infection. (**C**) Weight loss in mice that underwent bacterial pneumonia with or without rhACE2. (**D**) Bacterial load recovered from BALF. Final bacterial counts were normalized by recovery volume. (**E**) Neutrophil numbers in BALF were determined by flow cytometry gated as Ly-6G$^+$CD11b$^+$ in live cells (7AAD$^-$). (**F**–**I**) Proinflammatory cytokine and chemokine levels of CXCL5, G-CSF, Mip-2, and KC were determined by ELISA. (**J**) Representative micrograph of pathohistology of lungs from indicated groups at the time after bacterial inoculation. (**K** and **L**) Representative immunofluorescence images from an indicated experimental group of mice for iNOS (K) and neutrophil marker myeloperoxidase (MPO) (L). Data were analyzed for statistical significance by two-tailed Student *t* test using Prism software (GraphPad). In all experimental groups, $n \geq 4$. Scale bar, 50 μm. $^*p < 0.05$, $^{**}p < 0.01$, $^{***}p < 0.001$.

rhACE2 treatment after initial inflammatory response mitigates lung inflammation and injury in bacterial pneumonia

To reconcile the reported beneficial effect of rhACE2 with our observation that pretreatment of rhACE2 is detrimental, we next sought to evaluate whether restoration of ACE2 activity after initial inflammatory response to bacterial lung infection would dampen the inflammation and alleviate lung injury. To do so, we treated bacterially infected wild-type mice with rhACE2 (10 μg/kg) 24 h after *Pseudomonas* bacterial inoculation (Fig. 6A). As shown in Fig. 6, 48 h after bacterial lung infection, rhACE2 treatment is indeed beneficial as demonstrated as the improved bodyweight recovery (Fig. 6B), reduced lung permeability (Fig. 6C, 6D), mitigated neutrophil accumulation in mouse lungs (Fig. 6F), dampened inflammatory cytokine production (Fig. 6G, 6H), and alleviated inflammation and lung injury (Fig. 6I–L), although the bacterial burden in BALF was not changed (Fig. 6E). The results highlighted a therapeutic window to treat bacterial pneumonia by using recombinant active ACE2.

Pulmonary epithelial ACE2 is required to buffer exuberant neutrophilic lung inflammation in response to bacterial lung infection

In seeking to further understand the contributions of pulmonary ACE2 in the pathogenesis of bacterial pneumonia, we first screened ACE2 protein distribution in mouse lungs by immunofluorescence. As demonstrated in Fig. 7A and in Supplemental Fig. 1, ACE2 is predominantly expressed in cells in which transcriptional factor foxj1 is positive (foxj1$^+$), a marker for mature and ciliated lung epithelia. Accordingly, we generated a mouse line in which ACE2 is specifically deficient in foxj1$^+$ lung epithelia. The progeny, in this study called ACE2$^{\Delta foxj1}$ mice, were healthy, fertile, displayed no distinct lung phenotype, and reproduced at expected Mendelian ratios but exhibited reduced ACE2 expression and activity in the lung, confirming the success of the deletion strategy (Supplemental Fig. 2). When subjected to our bacterial pneumonia model, ACE2$^{\Delta foxj1}$ mice demonstrated a similar phenotype to what we observed in systemic ACE2-deficient mice (Fig. 2) as manifested by reduced survival rate (Fig. 7B), further weight loss (Fig. 7C), enhanced lung permeability (Fig. 7D, 7E), increased neutrophil infiltration (Fig. 7F), reduced bacterial outgrowth in BALF, exaggerated lung inflammation (Fig. 7H, 7I), and exacerbated lung injury (Fig. 7J–M), revealing that pulmonary epithelial ACE2 bears a relatively significant role in modulating neutrophil infiltration and lung inflammation in the disease setting.

ACE2 regulates IL-17–mediated neutrophil infiltration by modulating STAT3 signaling

It has been reported that IL-17 is critical in mediating pulmonary neutrophil infiltration, whereas the lungs encountered infectious insults (40–44). Our previous studies in necrotizing enterocolitis-induced lung injury also indicated that IL-17 is critical in neutrophilic lung inflammation (45). Thus, we hypothesized that IL-17–mediated neutrophil influx is, at least in part, the underlying mechanism by which ACE2 modulates neutrophilic

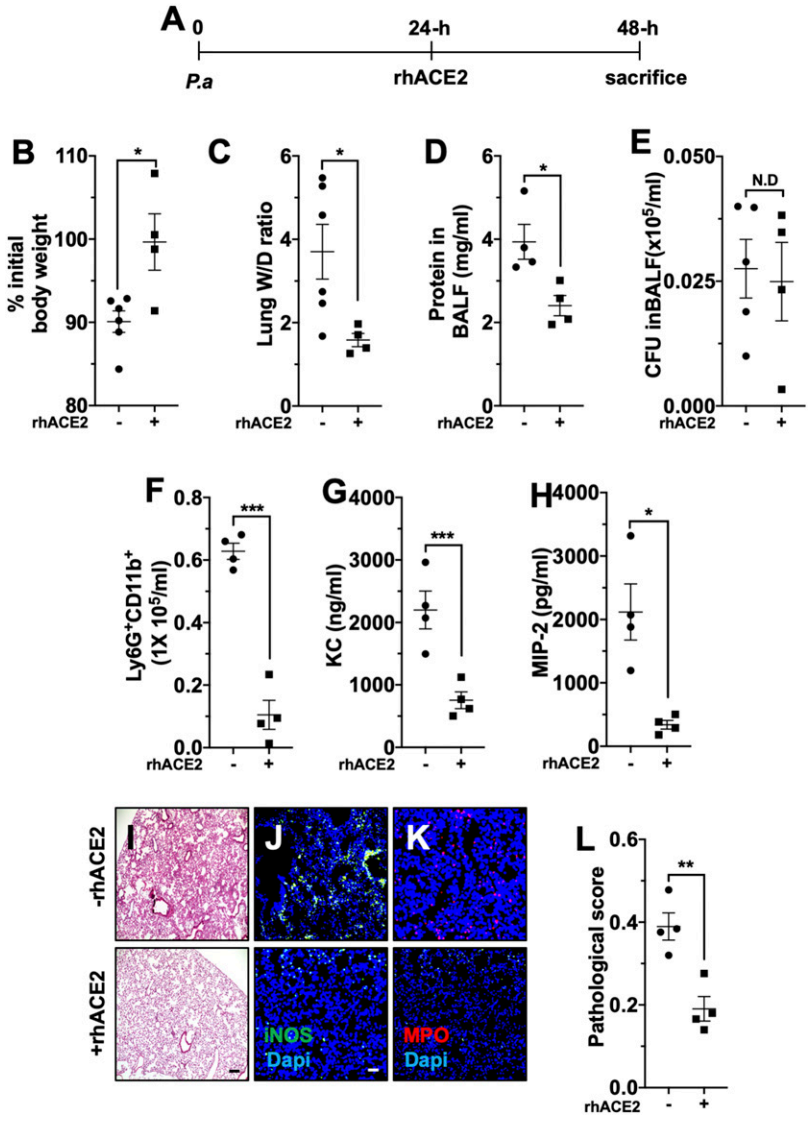

FIGURE 6. rhACE2 treatment after initial inflammatory response mitigates lung inflammation and injury in bacterial pneumonia. (**A**) Timeline depicting the experimental protocol. (**B**) Bodyweight changes relative to that before bacterial pneumonia model initiation with or without ACE2 intervention 48 h after bacterial inoculation. (**C**) The severity of lung edema in wild-type mice with or without recombinant ACE2 was determined by lung tissue wet/dry ratio measurement. (**D**) Protein levels in BALF from mice with or without rhACE2 was determined. (**E**) Bacterial load in BALF from mice of the individual experimental group was determined as CFU per milliliter. (**F**) The effect of recombinant ACE2 that was given after initial inflammatory process on the neutrophil accumulation in bacterially infected mouse lung was measured by flow cytometry as indicated as live Ly-6G$^+$CD11b$^+$ cells in BALF. (**G** and **H**) Active ACE2 enhancement led to reduced proinflammatory cytokine (Mip2 and KC) levels in BALF determined by ELISA. (**I**) Representative H&E staining micrographs are revealing histopathology in mouse lungs from respective experiment groups as indicated. (**J** and **K**) Representative immunofluorescence images from an indicated experimental group of mice for iNOS (J) and a marker of inflammation and neutrophil marker myeloperoxidase (MPO) (K). (**L**) Pathological scores of mouse lungs with or without recombinant ACE2 treatment after initial inflammation. Data were analyzed for statistical significance by two-tailed Student *t* test using Prism software (GraphPad). For each experimental group, $n \geq 4$. Scale bar, 50 μm. $^*p < 0.05$, $^{**}p < 0.01$, $^{***}p < 0.001$.

inflammation in bacterial lung infection. To test this hypothesis, we first measured IL-17A content in BALF from wild-type mice with or without *P. aeruginosa* instillation for 24 h. As shown in Fig. 8A, bacterial lung infection did induce IL-17A in mouse lung. Next, we administered the wild-type mice an ACE2-inhibitor MLN4760, and an IL-17A–neutralizing Ab by inhalation 2 h before and 24 h after *P. aeruginosa* inoculation. As indicated in Fig. 8B, ablating IL-17A in the lung precluded *P. aeruginosa* infection mediated neutrophil infiltration even in the presence of ACE2 inhibitor MLN4760, suggesting that ACE2 modulated neutrophil infiltration is, at least in part, through its effects on IL-17 signaling. Indeed, IL-17A induces more neutrophil infiltration in ACE2-deficient mice, and recombinant ACE2 significantly reduces IL-17A–mediated neutrophil infiltration (Fig. 8C). The results depicted in Fig. 8D, 8E indicated that recombinant ACE2 alleviated IL-17A–induced chemokine and cytokine levels in mouse lung BALF. To dissect how ACE2 affects IL-17 signaling, we first measured IL-17A levels in BALF from bacterially infected wild-type mice with manipulated ACE2 activity and from ACE2-deficient mice. As shown in Fig. 8F, IL-17A levels are not different in BALF from the mice in which pulmonary ACE2 were varied, indicating that the effect of ACE2 on IL-17–mediated neutrophil recruitment is not due to the impaired IL-17 production. Instead, it may be due to altered IL-17 signaling. To confirm this possibility, we detected a significant signaling molecule for IL-17–mediated neutrophil infiltration (46–50), STAT3, by Western blotting. As demonstrated, rhACE2 inhibited IL-17A–induced STAT3 phosphorylation both in vitro (cultured mouse lung organoids; Fig. 8G) and in vivo (mouse lung; Fig. 8H).

Moreover, we found that rhACE2 reduces STAT3 phosphorylation in the lung of wild-type and ACE2-deficient mice that underwent bacterial lung infection (Fig. 8I). Even more importantly, blocking STAT3 signaling by WP1066, a STAT3 inhibitor, resulted in the reduced neutrophil infiltration induced by a bacterial lung infection in the presence of ACE2-inhibitor MLN4760 (Fig. 8J). All the above observations suggest that ACE2 modulates neutrophil infiltration induced by a bacterial lung infection, in part, through regulating IL-17–mediated STAT3 signaling (Fig. 9).

Discussion

As summarized in Fig. 9, our current study reveals that the dynamic variation of pulmonary ACE2 is required to control the neutrophilic inflammation of the host in response to bacterial lung infection. Specifically, the initial reduction of pulmonary ACE2 while the host encounters a bacterial lung infection is crucial for recruiting the inflammatory neutrophils into the lung to combat the infection. However, the subsequent recovery of pulmonary ACE2 is equally

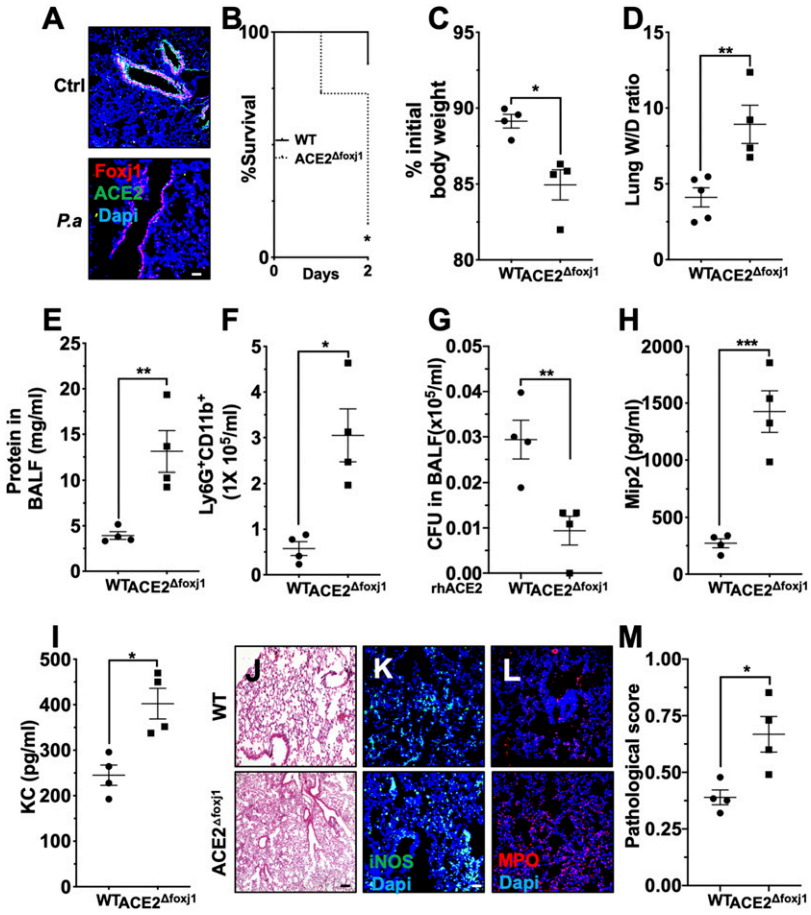

FIGURE 7. Pulmonary epithelial ACE2 is required to buffer exuberant neutrophilic lung inflammation in response to bacterial lung infection. (**A**) Representative images immunofluorescent staining for foxj1 (red) and ACE2 (green), demonstrating ACE2 is predominantly expressed in foxj1^{+} cells (upper panel), and the expression is reduced 48 h after bacterial infection (lower panel). (**B**) ACE2$^{\Delta foxj11}$ mice demonstrated more severe mortality in bacterial pneumonia (**C**). ACE2$^{\Delta foxj1}$ mice exhibited more weight loss in bacterial pneumonia in comparison with wild-type counterpart. (**D** and **E**) Bacterially infected ACE2$^{\Delta foxj1}$ mouse demonstrated an increased permeability as evidenced by elevated wet/dry ratio (D) and protein levels in BALF (E). (**F**) Neutrophil accumulation in ACE2$^{\Delta foxj1}$ mouse lung infected by *Pseudomonas* bacteria was exacerbated as manifested by increased Ly-6G^{+}CD11b^{+} live cells in BALF using flow cytometry. (**G**) Bacterial load in BALF from ACE2$^{\Delta foxj1}$ mouse lung infected by *Pseudomonas* bacteria was NS in comparison with that in the wild-type counterparts. (**H** and **I**) Excising ACE2 gene from foxj1^{+} cells led to enhanced proinflammatory cytokine production (KC and Mip2) as measured by ELISA. (**J**) Representative micrograph showing histology of lungs of ACE2$^{\Delta foxj1}$ mice with *Pseudomonas* bacterial infection. (**K** and **L**) Immunofluorescent images of inflammation marker iNOS (green) (K) and neutrophil marker myeloperoxidase (MPO; red) (L) in ACE2$^{\Delta foxj1}$ mice with a bacterial lung infection. (**M**) Pathological scores of mouse lungs from wild type and were calculated. Data were analyzed for statistical significance by two-tailed Student *t* test using Prism software (GraphPad). In all experimental groups, $n \geq 4$. Scale bar, 50 μm. $^{*}p < 0.05$, $^{**}p < 0.01$, $^{***}p < 0.001$.

critical to prohibit exuberant neutrophil accumulation and to safeguard the resolving process of lung inflammation. Confounding factors that either prevent the ACE2 dynamic from occurring or disrupt the dynamic are detrimental to the host, resulting in either compromised host-defense capability or heightened inflammatory response. These findings are significant to understand the biology of pulmonary ACE2 further and delineate the therapeutic potential of active ACE2 in infectious and inflammatory lung diseases.

Bacterial infections cause acute lung injury not only because of bacterial virulence but also because of the exaggerated inflammatory response of the susceptible host (28, 29). One of the essential initial components of the innate immune response against bacterial infection is the vigorous recruitment of neutrophils into the lungs (51, 52). Insufficient neutrophil recruitment will reduce bacterial clearance and result in more severe lung infection and higher mortality (30, 31). However, several life-threatening bacterial lung diseases are caused by excessive neutrophil-mediated inflammation (32, 33). Our results indicate that disrupting the ACE2 dynamic by keeping the active ACE2 level unchanged or even higher in bacterial lung infection impairs neutrophil influx and compromises host-defense capacity, leading to more severe lung infection and higher mortality (Fig. 5).

Inversely, altering the ACE2 dynamic by keeping the active pulmonary ACE2 at low levels led to exuberant neutrophilic accumulation in the lung, more severe lung injury, and worsened outcome (Fig. 2). More importantly, such an outcome is not due to compromised host-defense capacity, because the lack of active ACE2 reduced the bacterial burden in mouse lungs 48 h postinoculation. Instead, it results from exacerbated neutrophil infiltration and heightened inflammation. It is conceivable that a lack of active ACE2 mediated excessive accumulation of neutrophils in mouse lungs in response to a bacterial infection will enhance antimicrobial capacity if the bacterial killing capability of the accumulated neutrophils is not perturbed. However, exuberant neutrophilic infiltration will lead to heightened inflammatory response, more severe lung injury, and worsened outcome. Pre-existing and persistent deficiency of active ACE2 could happen in many physiological and pathological scenarios. For instance, it is reported that the expression of ACE2 gene is variable in the developing and aging lungs in comparison with mature adult lungs (33, 34). Many studies

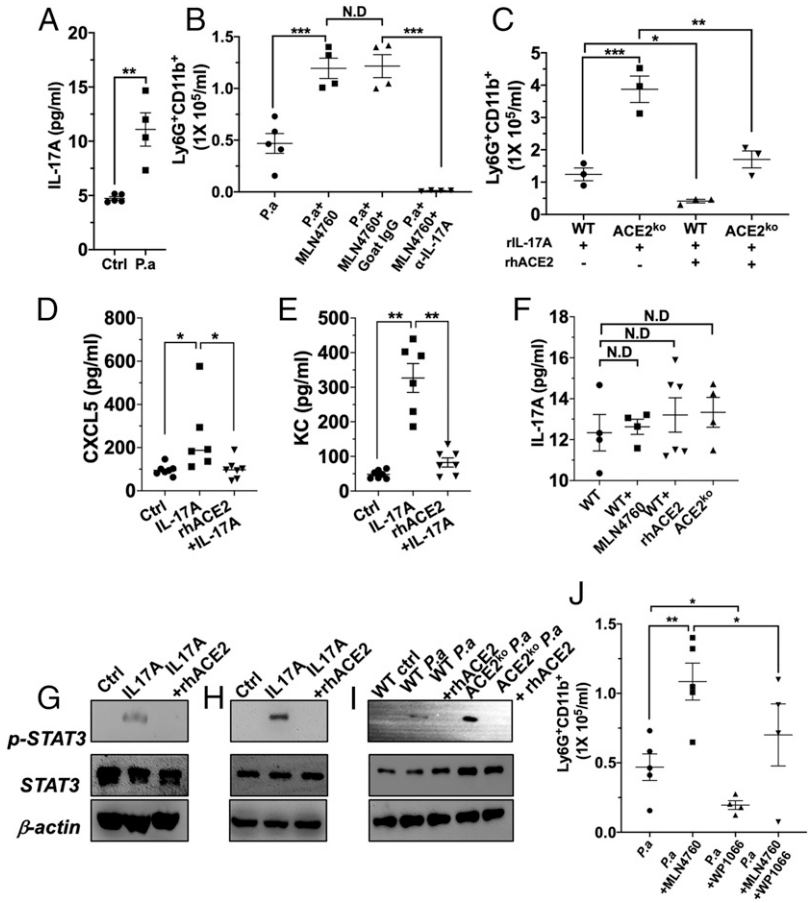

FIGURE 8. ACE2 regulates IL-17–mediated neutrophil infiltration by modulating STAT3 signaling. (**A**) IL-17A concentration in BALF from mice with or without *P. aeruginosa* lung infection was determined by ELISA. (**B**) Neutrophil counts in BALF from wild-type mice with *P. aeruginosa* lung infection with or without pre-existing reduced ACE2 and in the presence or absence of (A) IL-17A–neutralizing Ab. The neutrophils were detected by flow cytometry gated as Ly-6G$^+$CD11b$^+$ live cells. The counts were normalized with the volume of BALF in the individual experimental group of mice. (**C**) rIL-17A (100 ng/ml; 30 μl intranasal instillation) induces neutrophil infiltration in wild-type mice lungs, and the induction is more potent in ACE2-deficient mice. rhACE2 inhibits the IL-17A–induced neutrophil infiltration in mice (**D** and **E**). rhACE2 alleviates rIL-17–mediated cytokine and chemokine production in BALF. (**F**) IL-17A production in BALF from mice in which ACE2 activity was manipulated either by pharmacological reagents or by genetic modification. IL-17A concentration was determined by ELISA and normalized with respective BALF volume. (**G** and **H**) rhACE2 inhibited IL-17A–induced STAT3 phosphorylation in vitro (mouse lung organoids) (G) and in vivo (mouse lung) (H). (**I**) rhACE2 represses bacterial lung infection–induced STAT3 activation in both wild-type and ACE2-deficient mice. (**J**) Blocking STAT3 signaling alleviates the lack of pulmonary ACE2-induced exuberant neutrophil infiltration in bacterially infected mouse lung as manifested by Western blot for phosphorylated STAT3. WP1066, a STAT3 antagonist. Data were analyzed for statistical significance by two-tailed Student *t* test or ANOVA (ordinary one-way ANOVA multiple comparisons) using Prism software (GraphPad). In all experimental groups, $n \geq 3$. $^*p < 0.05$, $^{**}p < 0.01$, $^{***}p < 0.001$.

revealed that viral infection could inhibit ACE2 gene expression in the lung. Thus, the state of active ACE2 at the time of subsequent bacterial lung infection might, in part, determine the disease outcome.

The balance between pro- and anti-inflammatory signals will determine whether recovery or deterioration will occur after exposure to pathogenic insults. Our findings show that interruption of the active ACE2 recovery after bacterial lung infection delays the resolving process of lung inflammation (Fig. 4); therefore, it has significant clinical relevance because bacterial lung infection could be a symbiotic disease associated with smoking, combined viral-bacterial lung infection and trauma (38–41), conditions that may attenuate ACE2 recovery and perturb the resolution of lung inflammation, all of which lead to chronic lung inflammation and injury.

Interestingly, we found a therapeutic window for primary bacterial pneumonia by enhancing pulmonary ACE2 activity using recombinant ACE2. Our findings indicate that recombinant ACE2 could be used to treat bacterial pneumonia after an initial inflammatory response has occurred to alleviate lung inflammation and injury while keeping the host-defense capability uncompromised (Fig. 6). A few reports demonstrated the beneficial effect of enhancing ACE2 activity either by recombinant ACE2 or by an ACE2 activator, such as diminazene aceturate, in a variety of disease models (39, 53–56). For instance, rhACE2 has been tested in a clinical trial to treat adult respiratory distress syndrome patients. However, preliminary results from the trial showed only a minimal beneficial effect of such a strategy on the outcome of adult respiratory distress syndrome patients despite significant surfactant D increase and trend of IL-6 decrease in plasma (57). According to our current study, future clinical trials need to consider both the state of ACE2 activity and the state of inflammation at the time of intervention to achieve optimal beneficial therapy and to avoid detrimental side effects.

Previously, we reported that ACE2 is predominantly expressed in mature, ciliated-airway epithelia in humans, which are foxj1 transcription factor–expressing cells (42). Our immunofluorescence staining result indicated that ACE2 is also expressed in

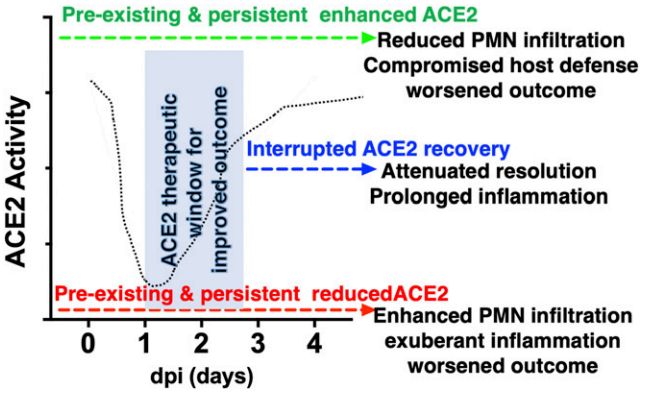

FIGURE 9. Schematic of the working hypothesis delineating the role of ACE2 to modulate neutrophilic inflammation in a bacterial pneumonia mouse model. Bacterial lung infection leads to pulmonary dynamic variation, which is required to modulate neutrophil influx. Pre-existing and persistent enhanced or reduced levels of active ACE2 that disrupts ACE2 dynamic during bacterial pneumonia results in a worsened outcome. Also, interrupted ACE2 recovery delays the resolution process of neutrophilia and lung inflammation in bacterial pneumonia. However, a therapeutic window for the improved outcome using active ACE2 is tangible.

the foxj1$^+$ cells of airway epithelia in mouse (Supplemental Fig. 1). Deleting the ACE2 gene from mouse lung foxj1$^+$ cell resulted in reduced ACE2 activity in BALF (Supplemental Fig. 2), and the mice exhibited enhanced inflammatory response to bacterial lung infection, which resembles the inflammatory response in bacterially infected mouse lungs we observed in global ACE2-deficient mice, confirming that the pulmonary epithelial ACE2 played critical role in this disease setting (Fig. 7). Of note, the active ACE2 we measured in the current study reflects only the soluble form of ACE2, which is produced by ACE2 sheddase, namely ADAM17, from ACE2-expressing cells (34, 58). The dynamic change and role of cell membrane–bound versus soluble ACE2 in the pathogenesis of bacterial pneumonia needs to be further investigated to understand ACE2 biology in the lung better.

IL-17 is produced by several innate and adaptive immune cells, including Th17 cells, NKT cells, CD8$^+$ T cells, γδ T cells, and innate lymphoid three cells (ILC3) (59–63). It has been reported that IL-17 plays a pivotal role in recruiting neutrophils via the CXC chemokine to induce the chemotaxis and accumulation of inflammatory cells, such as neutrophils, to the sites of inflammation (64–67). Accumulating evidence indicated that Gram-negative bacteria appear to induce the expression of IL-17 via IL-23 and TLR4 (68). However, IL-17 does not directly promote chemotaxis. Instead, it promotes the release of recruitment factors from the inflamed microenvironment (69, 70). Our novel observation that ACE2 modulates *P. aeruginosa*–induced neutrophil infiltration in mouse lung through regulating the IL-17 signaling is thus in agreement with those previous studies. To the best of our knowledge, the current study is the first to link pulmonary ACE2, IL-17, and neutrophil accumulation in bacterial lung infection setting. Remarkably, we demonstrated that ACE2 does not affect the production of IL-17 but rather that ACE2 regulates IL-17 signaling. The activation of STAT3 signaling is crucial to induce CD4$^+$ T cell differentiation toward Th17 lineage (71); however, many IL-17–mediated effects depend on STAT3 activity (72–74). Thus, our observation suggests that ACE2 has little or no effects on CD4$^+$ T cell polarization toward the Th17 subset. Instead, ACE2 might influence IL-17 signaling through its impact on STAT3 activation. Studies have shown that inhibitors of STAT3 can be effective in the treatment of inflammatory diseases. Our results indicate that ACE2 suppresses neutrophilic inflammation by inhibiting IL-17 responses and that STAT3 signaling is associated with this process. Although our current study confirmed several previous reports that suggested that STAT3 signaling is proinflammatory, few studies indicated that inhibiting STAT3 pathway amplifies the inflammatory response in a sepsis mouse model (75). The discrepancy might be attributed to the distinct animal strains and variable inducers of inflammation in different models.

We acknowledge that the current study has limitations. First, we only used a single strain of bacteria in our model. The role of ACE2 in other infectious lung disease models (such as a porcine model of *Staphylococcus* bacterial lung infection) needs to be verified. Second, mouse lung is quite different from human lung, and a mouse model of a bacterial lung infection cannot fully mimic the state of bacterial lung infection in human. Our results need to be tested in more clinically relevant animal models, such as pig bacterial lung infection models.

Taken together, our current study demonstrates a critical role of active ACE2 in modulating the innate immune response to bacterial lung infection by regulating proinflammatory neutrophil influx. Importantly, our study highlights several therapeutic windows and strategies by manipulating active ACE2 to optimize the host-defense capability and to alleviate inflammatory lung disease and injury in the setting of bacterial lung infection.

Disclosures

The authors have no financial conflicts of interest.

References

1. Bijani, B., H. Mozhdehipanah, H. Jahanihashemi, and S. Azizi. 2014. The impact of pneumonia on hospital stay among patients hospitalized for acute stroke. *Neurosciences (Riyadh)* 19: 118–123.
2. Chow, E. J., and L. A. Mermel. 2017. Hospital-acquired respiratory viral infections: incidence, morbidity, and mortality in pediatric and adult patients. *Open Forum Infect. Dis.* 4: ofx006.
3. Chughtai, M., C. U. Gwam, N. Mohamed, A. Khlopas, J. M. Newman, R. Khan, A. Nadhim, S. Shaffiy, and M. A. Mont. 2017. The epidemiology and risk factors for postoperative pneumonia. *J. Clin. Med. Res.* 9: 466–475.
4. Li, H., and B. Cao. 2017. Pandemic and avian influenza a viruses in humans: epidemiology, virology, clinical characteristics, and treatment strategy. *Clin. Chest Med.* 38: 59–70.
5. Dick, A., H. Liu, J. Zwanziger, E. Perencevich, E. Y. Furuya, E. Larson, M. Pogorzelska-Maziarz, and P. W. Stone. 2012. Long-term survival and healthcare utilization outcomes attributable to sepsis and pneumonia. *BMC Health Serv. Res.* 12: 432.
6. Cassiere, H. A., and A. M. Fein. 1996. Severe community-acquired pneumonia. *Curr. Opin. Pulm. Med.* 2: 186–191.
7. Cilloniz, C., I. Martin-Loeches, C. Garcia-Vidal, A. San Jose, and A. Torres. 2016. Microbial etiology of pneumonia: epidemiology, diagnosis and resistance patterns. *Int. J. Mol. Sci.* 17: 2120.
8. Zilberberg, M. D., and A. F. Shorr. 2013. Prevalence of multidrug-resistant *Pseudomonas aeruginosa* and carbapenem-resistant Enterobacteriaceae among specimens from hospitalized patients with pneumonia and bloodstream infections in the United States from 2000 to 2009. *J. Hosp. Med.* 8: 559–563.
9. Cantone, M., G. Santos, P. Wentker, X. Lai, and J. Vera. 2017. Multiplicity of mathematical modeling strategies to search for molecular and cellular insights into bacteria lung infection. [Published erratum appears in 2017 *Front. Physiol.* 8: 817.] *Front. Physiol.* 8: 645.
10. Lawrence, D. W., and J. Kornbluth. 2018. Reduced inflammation and cytokine production in NKLAM deficient mice during *Streptococcus pneumoniae* infection. *PLoS One* 13: e0194202.
11. Robinson, K. M., K. Ramanan, M. E. Clay, K. J. McHugh, M. J. Pilewski, K. L. Nickolich, C. Corey, S. Shiva, J. Wang, R. Muzumdar, and J. F. Alcorn. 2018. The inflammasome potentiates influenza/*Staphylococcus aureus* superinfection in mice. *JCI Insight* 3: e97470.
12. Mirabito Colafella, K. M., D. M. Bovée, and A. H. J. Danser. 2019. The renin-angiotensin-aldosterone system and its therapeutic targets. *Exp. Eye Res.* 186: 107680.
13. Mowry, F. E., and V. C. Biancardi. 2019. Neuroinflammation in hypertension: the renin-angiotensin system versus pro-resolution pathways. *Pharmacol. Res.* 144: 279–291.
14. Rivière, G., A. Michaud, C. Breton, G. VanCamp, C. Laborie, M. Enache, J. Lesage, S. Deloof, P. Corvol, and D. Vieau. 2005. Angiotensin-converting

enzyme 2 (ACE2) and ACE activities display tissue-specific sensitivity to undernutrition-programmed hypertension in the adult rat. *Hypertension* 46: 1169–1174.
15. Schütz, S., J. M. Le Moullec, P. Corvol, and J. M. Gasc. 1996. Early expression of all the components of the renin-angiotensin-system in human development. *Am. J. Pathol.* 149: 2067–2079.
16. Hilgenfeldt, U., G. Kienapfel, W. Kellermann, R. Schott, and M. Schmidt. 1987. Renin-angiotensin system in sepsis. *Clin. Exp. Hypertens. A* 9: 1493–1504.
17. Kim, J., J. K. Lee, E. Y. Heo, H. S. Chung, and D. K. Kim. 2016. The association of renin-angiotensin system blockades and pneumonia requiring admission in patients with COPD. *Int. J. Chron. Obstruct. Pulmon. Dis.* 11: 2159–2166.
18. Ding, C., C. van 't Veer, J. J. T. H. Roelofs, M. Shukla, K. R. McCrae, A. S. Revenko, J. Crosby, and T. van der Poll. 2018. Limited role of kininogen in the host response during gram-negative pneumonia-derived sepsis. *Am. J. Physiol. Lung Cell. Mol. Physiol.* 314: L397–L405.
19. Perevozchikov, P. N., and V. F. Cheganov. 1988. [Parasympathetic component of the regulation of the kallikrein-kinin system in experimental pneumonia]. *Biull. Eksp. Biol. Med.* 106: 417–419.
20. Jia, H. 2016. Pulmonary angiotensin-converting enzyme 2 (ACE2) and inflammatory lung disease. *Shock* 46: 239–248.
21. Kuba, K., Y. Imai, S. Rao, H. Gao, F. Guo, B. Guan, Y. Huan, P. Yang, Y. Zhang, W. Deng, et al. 2005. A crucial role of angiotensin converting enzyme 2 (ACE2) in SARS coronavirus-induced lung injury. *Nat. Med.* 11: 875–879.
22. Shi, Y., B. Zhang, X. J. Chen, D. Q. Xu, Y. X. Wang, H. Y. Dong, S. R. Ma, R. H. Sun, Y. P. Hui, and Z. C. Li. 2013. Osthole protects lipopolysaccharide-induced acute lung injury in mice by preventing down-regulation of angiotensin-converting enzyme 2. *Eur. J. Pharm. Sci.* 48: 819–824.
23. Lambert, D. W., N. M. Hooper, and A. J. Turner. 2008. Angiotensin-converting enzyme 2 and new insights into the renin-angiotensin system. *Biochem. Pharmacol.* 75: 781–786.
24. Turner, A. J., S. R. Tipnis, J. L. Guy, G. Rice, and N. M. Hooper. 2002. ACEH/ACE2 is a novel mammalian metallocarboxypeptidase and a homologue of angiotensin-converting enzyme insensitive to ACE inhibitors. *Can. J. Physiol. Pharmacol.* 80: 346–353.
25. Imai, Y., K. Kuba, S. Rao, Y. Huan, F. Guo, B. Guan, P. Yang, R. Sarao, T. Wada, H. Leong-Poi, et al. 2005. Angiotensin-converting enzyme 2 protects from severe acute lung failure. *Nature* 436: 112–116.
26. Gaddam, R. R., S. Chambers, and M. Bhatia. 2014. ACE and ACE2 in inflammation: a tale of two enzymes. *Inflamm. Allergy Drug Targets* 13: 224–234.
27. Liu, Q., J. Du, X. Yu, J. Xu, F. Huang, X. Li, C. Zhang, X. Li, J. Chang, D. Shang, et al. 2017. miRNA-200c-3p is crucial in acute respiratory distress syndrome. *Cell Discov.* 3: 17021.
28. Sodhi, C. P., C. Wohlford-Lenane, Y. Yamaguchi, T. Prindle, W. B. Fulton, S. Wang, P. B. McCray, Jr., M. Chappell, D. J. Hackam, and H. Jia. 2018. Attenuation of pulmonary ACE2 activity impairs inactivation of des-Arg^9 bradykinin/BKB1R axis and facilitates LPS-induced neutrophil infiltration. *Am. J. Physiol. Lung Cell. Mol. Physiol.* 314: L17–L31.
29. Zhang, Y., G. Huang, L. P. Shornick, W. T. Roswit, J. M. Shipley, S. L. Brody, and M. J. Holtzman. 2007. A transgenic FOXJ1-Cre system for gene inactivation in ciliated epithelial cells. *Am. J. Respir. Cell Mol. Biol.* 36: 515–519.
30. Hild, M., and A. B. Jaffe. 2016. Production of 3-D airway organoids from primary human airway basal cells and their use in high-throughput screening. *Curr. Protoc. Stem Cell Biol.* 37: IE.9.1–IE.9.15.
31. Tan, Q., K. M. Choi, D. Sicard, and D. J. Tschumperlin. 2017. Human airway organoid engineering as a step toward lung regeneration and disease modeling. *Biomaterials* 113: 118–132.
32. Cetin, S., H. R. Ford, L. R. Sysko, C. Agarwal, J. Wang, M. D. Neal, C. Baty, G. Apodaca, and D. J. Hackam. 2004. Endotoxin inhibits intestinal epithelial restitution through activation of Rho-GTPase and increased focal adhesions. *J. Biol. Chem.* 279: 24592–24600.
33. Egan, C. E., C. P. Sodhi, M. Good, J. Lin, H. Jia, Y. Yamaguchi, P. Lu, C. Ma, M. F. Branca, S. Weyandt, et al. 2016. Toll-like receptor 4-mediated lymphocyte influx induces neonatal necrotizing enterocolitis. *J. Clin. Invest.* 126: 495–508.
34. Jia, H. P., D. C. Look, P. Tan, L. Shi, M. Hickey, L. Gakhar, M. C. Chappell, C. Wohlford-Lenane, and P. B. McCray, Jr. 2009. Ectodomain shedding of angiotensin converting enzyme 2 in human airway epithelia. *Am. J. Physiol. Lung Cell. Mol. Physiol.* 297: L84–L96.
35. Yang, P., H. Gu, Z. Zhao, W. Wang, B. Cao, C. Lai, X. Yang, L. Zhang, Y. Duan, S. Zhang, et al. 2014. Angiotensin-converting enzyme 2 (ACE2) mediates influenza H7N9 virus-induced acute lung injury. *Sci. Rep.* 4: 7027.
36. Zou, Z., Y. Yan, Y. Shu, R. Gao, Y. Sun, X. Li, X. Ju, Z. Liang, Q. Liu, Y. Zhao, et al. 2014. Angiotensin-converting enzyme 2 protects from lethal avian influenza A H5N1 infections. *Nat. Commun.* 5: 3594.
37. Zhang, H., and A. Baker. 2017. Recombinant human ACE2: acing out angiotensin II in ARDS therapy. *Crit. Care* 21: 305.
38. Li, S. M., X. Y. Wang, F. Liu, and X. H. Yang. 2018. [ACE2 agonist DIZE alleviates lung injury induced by limb ischemia-reperfusion in mice]. *Sheng Li Xue Bao* 70: 175–183.
39. Tan, W. S. D., W. Liao, S. Zhou, D. Mei, and W. F. Wong. 2018. Targeting the renin-angiotensin system as novel therapeutic strategy for pulmonary diseases. *Curr. Opin. Pharmacol.* 40: 9–17.
40. McCarthy, M. K., L. Zhu, M. C. Procario, and J. B. Weinberg. 2014. IL-17 contributes to neutrophil recruitment but not to control of viral replication during acute mouse adenovirus type 1 respiratory infection. *Virology* 456–457: 259–267.
41. Roos, A. B., S. Sethi, J. Nikota, C. T. Wrona, M. G. Dorrington, C. Sandén, C. M. Bauer, P. Shen, D. Bowdish, C. S. Stevenson, et al. 2015. IL-17A and the promotion of neutrophilia in acute exacerbation of chronic obstructive pulmonary disease. *Am. J. Respir. Crit. Care Med.* 192: 428–437.
42. Li, X., S. He, R. Li, X. Zhou, S. Zhang, M. Yu, Y. Ye, Y. Wang, C. Huang, and M. Wu. 2016. *Pseudomonas aeruginosa* infection augments inflammation through miR-301b repression of c-Myb-mediated immune activation and infiltration. *Nat. Microbiol.* 1: 16132.
43. Mize, M. T., X. L. Sun, and J. W. Simecka. 2018. Interleukin-17A exacerbates disease severity in BALB/c mice susceptible to lung infection with *mycoplasma* pulmonis. *Infect. Immun.* 86: e00292-18.
44. Qiao, S., H. Zhang, X. Zha, W. Niu, J. Liang, G. Pang, Y. Tang, T. Liu, H. Zhao, Y. Wang, and H. Bai. 2019. Endogenous IL-17A mediated neutrophil infiltration by promoting chemokines expression during chlamydial lung infection. *Microb. Pathog.* 129: 106–111.
45. Jia, H., C. P. Sodhi, Y. Yamaguchi, P. Lu, M. R. Ladd, A. Werts, W. B. Fulton, S. Wang, T. Prindle, Jr., and D. J. Hackam. 2019. Toll like receptor 4 mediated lymphocyte imbalance induces Nec-induced lung injury. *Shock* 52: 215–223.
46. Fogli, L. K., M. S. Sundrud, S. Goel, S. Bajwa, K. Jensen, E. Derudder, A. Sun, M. Coffre, C. Uyttenhove, J. Van Snick, et al. 2013. T cell-derived IL-17 mediates epithelial changes in the airway and drives pulmonary neutrophilia. [Published erratum appears in 2013 *J. Immunol.* 191: 5318.] *J. Immunol.* 191: 3100–3111.
47. Zhang, Y., L. Zhang, J. Wu, C. Di, and Z. Xia. 2013. Heme oxygenase-1 exerts a protective role in ovalbumin-induced neutrophilic airway inflammation by inhibiting Th17 cell-mediated immune response. *J. Biol. Chem.* 288: 34612–34626.
48. Yan, Z., Z. Xiaoyu, S. Zhixin, Q. Di, D. Xinyu, X. Jing, H. Jing, D. Wang, Z. Xi, Z. Chunrong, and W. Daoxin. 2016. Rapamycin attenuates acute lung injury induced by LPS through inhibition of Th17 cell proliferation in mice. *Sci. Rep.* 6: 20156.
49. Ding, F. M., R. M. Liao, Y. Q. Chen, G. G. Xie, P. Y. Zhang, P. Shao, and M. Zhang. 2017. Upregulation of SOCS3 in lung CD4+ T cells in a mouse model of chronic PA lung infection and suppression of Th17-mediated neutrophil recruitment in exogenous SOCS3 transfer in vitro. *Mol. Med. Rep.* 16: 778–786.
50. Ding, F. M., X. Y. Zhang, Y. Q. Chen, R. M. Liao, G. G. Xie, P. Y. Zhang, P. Shao, and M. Zhang. 2018. Lentivirus-mediated overexpression of suppressor of cytokine signaling-3 reduces neutrophilic airway inflammation by suppressing T-helper 17 responses in mice with chronic *Pseudomonas aeruginosa* lung infections. *Int. J. Mol. Med.* 41: 2193–2200.
51. Tateda, K., T. A. Moore, J. C. Deng, M. W. Newstead, X. Zeng, A. Matsukawa, M. S. Swanson, K. Yamaguchi, and T. J. Standiford. 2001. Early recruitment of neutrophils determines subsequent T1/T2 host responses in a murine model of *Legionella pneumophila* pneumonia. *J. Immunol.* 166: 3355–3361.
52. Xu, N., X. P. Gao, R. D. Minshall, A. Rahman, and A. B. Malik. 2002. Time-dependent reversal of sepsis-induced PMN uptake and lung vascular injury by expression of CD18 antagonist. *Am. J. Physiol. Lung Cell. Mol. Physiol.* 282: L796–L802.
53. Shenoy, V., Y. Qi, M. J. Katovich, and M. K. Raizada. 2011. ACE2, a promising therapeutic target for pulmonary hypertension. *Curr. Opin. Pharmacol.* 11: 150–155.
54. Dhawale, V. S., V. R. Amara, P. A. Karpe, V. Malek, D. Patel, and K. Tikoo. 2016. Activation of angiotensin-converting enzyme 2 (ACE2) attenuates allergic airway inflammation in rat asthma model. *Toxicol. Appl. Pharmacol.* 306: 17–26.
55. Gu, H., Z. Xie, T. Li, S. Zhang, C. Lai, P. Zhu, K. Wang, L. Han, Y. Duan, Z. Zhao, et al. 2016. Angiotensin-converting enzyme 2 inhibits lung injury induced by respiratory syncytial virus. *Sci. Rep.* 6: 19840.
56. Rathinasabapathy, A., A. J. Bryant, T. Suzuki, C. Moore, S. Shay, S. Gladson, J. D. West, and E. J. Carrier. 2018. rhACE2 therapy modifies bleomycin-induced pulmonary hypertension via rescue of vascular remodeling. *Front. Physiol.* 9: 271.
57. Khan, A., C. Benthin, B. Zeno, T. E. Albertson, J. Boyd, J. D. Christie, R. Hall, G. Poirier, J. J. Ronco, M. Tidswell, et al. 2017. A pilot clinical trial of recombinant human angiotensin-converting enzyme 2 in acute respiratory distress syndrome. *Crit. Care* 21: 234.
58. Lambert, D. W., M. Yarski, F. J. Warner, P. Thornhill, E. T. Parkin, A. I. Smith, N. M. Hooper, and A. J. Turner. 2005. Tumor necrosis factor-alpha convertase (ADAM17) mediates regulated ectodomain shedding of the severe-acute respiratory syndrome-coronavirus (SARS-CoV) receptor, angiotensin-converting enzyme-2 (ACE2). *J. Biol. Chem.* 280: 30113–30119.
59. Park, H., Z. Li, X. O. Yang, S. H. Chang, R. Nurieva, Y. H. Wang, Y. Wang, L. Hood, Z. Zhu, Q. Tian, and C. Dong. 2005. A distinct lineage of CD4 T cells regulates tissue inflammation by producing interleukin 17. *Nat. Immunol.* 6: 1133–1141.
60. Aujla, S. J., P. J. Dubin, and J. K. Kolls. 2007. Interleukin-17 in pulmonary host defense. *Exp. Lung Res.* 33: 507–518.
61. Li, P., Q. Z. Yang, W. Wang, G. Q. Zhang, and J. Yang. 2018. Increased IL-4- and IL-17-producing CD8$^+$ cells are related to decreased CD39$^+$CD4$^+$Foxp3$^+$ cells in allergic asthma. *J. Asthma* 55: 8–14.
62. Sun, L. D., S. Qiao, Y. Wang, G. J. Pang, X. Y. Zha, T. L. Liu, H. L. Zhao, J. Y. Liang, N. B. Zheng, L. Tan, et al. 2018. Vγ4+ T cells: a novel IL-17-producing γδ T subsets during the early phase of chlamydial airway infection in mice. *Mediators Inflamm.* 2018: 6265746.
63. Cai, T., J. Qiu, Y. Ji, W. Li, Z. Ding, C. Suo, J. Chang, J. Wang, R. He, Y. Qian, et al. 2019. IL-17-producing ST2$^+$ group 2 innate lymphoid cells play a pathogenic role in lung inflammation. *J. Allergy Clin. Immunol.* 143: 229–244.e9.
64. Ruddy, M. J., F. Shen, J. B. Smith, A. Sharma, and S. L. Gaffen. 2004. Interleukin-17 regulates expression of the CXC chemokine LIX/CXCL5 in osteoblasts: implications for inflammation and neutrophil recruitment. *J. Leukoc. Biol.* 76: 135–144.

65. Griffin, G. K., G. Newton, M. L. Tarrio, D. X. Bu, E. Maganto-Garcia, V. Azcutia, P. Alcaide, N. Grabie, F. W. Luscinskas, K. J. Croce, and A. H. Lichtman. 2012. IL-17 and TNF-α sustain neutrophil recruitment during inflammation through synergistic effects on endothelial activation. *J. Immunol.* 188: 6287–6299.
66. Yuan, S., S. Zhang, Y. Zhuang, H. Zhang, J. Bai, and Q. Hou. 2015. Interleukin-17 stimulates STAT3-mediated endothelial cell activation for neutrophil recruitment. *Cell. Physiol. Biochem.* 36: 2340–2356.
67. Veres, T. Z., T. Kopcsányi, N. van Panhuys, M. Y. Gerner, Z. Liu, P. Rantakari, J. Dunkel, M. Miyasaka, M. Salmi, S. Jalkanen, and R. N. Germain. 2017. Allergen-induced CD4+ T cell cytokine production within airway mucosal dendritic cell-T cell clusters drives the local recruitment of myeloid effector cells. *J. Immunol.* 198: 895–907.
68. Zhu, H., J. Li, S. Wang, K. Liu, L. Wang, and L. Huang. 2013. Hmgb1-TLR4-IL-23-IL-17A axis promote ischemia-reperfusion injury in a cardiac transplantation model. *Transplantation* 95: 1448–1454.
69. Laan, M., Z. H. Cui, H. Hoshino, J. Lötvall, M. Sjöstrand, D. C. Gruenert, B. E. Skoogh, and A. Lindén. 1999. Neutrophil recruitment by human IL-17 via C-X-C chemokine release in the airways. *J. Immunol.* 162: 2347–2352.
70. Lindén, A. 2001. Role of interleukin-17 and the neutrophil in asthma. *Int. Arch. Allergy Immunol.* 126: 179–184.
71. Nishihara, M., H. Ogura, N. Ueda, M. Tsuruoka, C. Kitabayashi, F. Tsuji, H. Aono, K. Ishihara, E. Huseby, U. A. Betz, et al. 2007. IL-6-gp130-STAT3 in T cells directs the development of IL-17+ Th with a minimum effect on that of Treg in the steady state. *Int. Immunol.* 19: 695–702.
72. Wilson, R. P., M. L. Ives, G. Rao, A. Lau, K. Payne, M. Kobayashi, P. D. Arkwright, J. Peake, M. Wong, S. Adelstein, et al. 2015. STAT3 is a critical cell-intrinsic regulator of human unconventional T cell numbers and function. *J. Exp. Med.* 212: 855–864.
73. Su, S. A., D. Yang, W. Zhu, Z. Cai, N. Zhang, L. Zhao, J. A. Wang, and M. Xiang. 2016. Interleukin-17A mediates cardiomyocyte apoptosis through Stat3-iNOS pathway. *Biochim. Biophys. Acta* 1863: 2784–2794.
74. Ma, M., W. Huang, and D. Kong. 2018. IL-17 inhibits the accumulation of myeloid-derived suppressor cells in breast cancer via activating STAT3. *Int. Immunopharmacol.* 59: 148–156.
75. Williamson, L., I. Ayalon, H. Shen, and J. Kaplan. 2019. Hepatic STAT3 inhibition amplifies the inflammatory response in obese mice during sepsis. *Am. J. Physiol. Endocrinol. Metab.* 316: E286–E292.